Research Article

Study of the Performance of the Organic Extracts of *Chenopodium ambrosioides* for Ag Nanoparticle Synthesis

Luis M. Carrillo-López,[1] Ramón M. Soto-Hernández,[2] Hilda A. Zavaleta-Mancera,[2] and Alfredo R. Vilchis-Néstor[3]

[1]*Facultad de Zootecnia y Ecología, CONACYT-Universidad Autónoma de Chihuahua, 31453 Chihuahua, CHIH, Mexico*
[2]*Botánica, Colegio de Postgraduados, 56230 Texcoco, MEX, Mexico*
[3]*Centro Conjunto de Investigación en Química Sustentable UAEM-UNAM, 50200 Toluca, MEX, Mexico*

Correspondence should be addressed to Luis M. Carrillo-López; luismanuel@colpos.mx

There are many ways to obtain metal nanoparticles: biological, physical, and chemical ways and combinations of these approaches. Synthesis assisted with plant extracts has been widely documented. However, one issue that is under discussion refers to the metabolites responsible for reduction and stabilization that confine nanoparticle growth and prevent coalescence between nanoparticles in order to avoid agglomeration/precipitation. In this study, Ag nanoparticles were synthesized using organic extracts of *Chenopodium ambrosioides* with different polarities (hexane, dichloromethane, and methanol). Each extract was phytochemically characterized to identify the nature of the metabolites responsible for nanoparticle formation. With methanol extract, the compounds responsible for reducing and stabilizing silver nanoparticle were associated with the presence of phenolic compounds (flavonoids and tannins), while, with dichloromethane and hexane extracts, the responsible compounds were mainly terpenoids. Large part of the reducing activity of secondary metabolites in *C. ambrosioides* is closely related to compounds with antioxidant capacity, such as phenolic compounds (flavone glycoside and isorhamnetin), which are the main constituents of the methanol extracts. Otherwise, terpenoids (trans-diol, α-terpineol, monoterpene hydroperoxides, and apiole) are the central metabolites present in dichloromethane and hexane extracts.

1. Introduction

Nanoparticles, with their different morphologies and sizes, have been of growing interest because of their properties, among which is their mass/volume ratio, which is different from that of matter in bulk. Chemical and physical methods of synthesis are the traditional methods, but their disadvantage is the use of chemicals that are toxic for the environment. Biological methods include the use of plants as well as other organisms such as bacteria and fungi. Biological synthesis is a relatively easy and versatile technique, quite attractive for medical applications, because nanoparticle formation employs natural molecules that are abundant in plants. The reducing properties of plant extracts and their constituents, such as flavanones and terpenoids, play a crucial role in the reduction process of metallic ions to nanoparticles [1].

C. ambrosioides is an odorous ruderal arvensis native of South America and Mexico and naturalized in hot and temperate regions of the Old World [2]. In Mexico, its distribution includes 29 of the country's 31 states [3]. The extensive uses of the genus *Chenopodium* in traditional medicine have resulted in considerable chemical analyses of the plants and their active principles. Phytochemical research on the genus *Chenopodium* has come up with compounds with a vast variety of structural patterns such as primary metabolites (carbohydrates, amino acids, nonpolar constituents, proteins, aromatic cytokinins, and hormones) and secondary metabolites (flavonoids, saponins, terpenes, sterols, and alkaloids).

Titrimetric trials have been used for preliminary evaluation of the reducing potential of different medicinal plant species. *Eucalyptus camaldulensis* has a KOE (amount

in mg of $KMnO_4$ used to oxidize 1 mg of dry extract) of 2.6 and *Pelargonium roseum* with a KOE of 3.29. Both species had high reducing potential. For this reason, their methanol extracts were used for metal nanoparticle synthesis. The reducing ability of the extracts was significantly higher than that of *Azadirachta indica*, used as the control (KOE = 1.2). *E. camaldulensis* and *P. roseum* produced gold nanoparticles of 1.25–17.5 nm and 2.5–27.5 nm, with average sizes of 5.5 nm and 7.5 nm, respectively [4]. Au nanoparticles produced with extracts of *Magnolia Kobus* were coated with proteins and other biomolecules such as terpenoids with functional groups of amine, aldehydes, carboxyl, and alcohols that play a vital role in nanoparticle synthesis [5]. A more specific study on *C. ambrosioides* detailed the following metabolites: hexoses (glucose), amino acids (alanine, glycine, valine, and leucine), phenolics (flavonoids such as flavone glycoside, kaempferol), sterols, monoterpenoids (*b*-myrcene, *cis-b*-ocimene, nerol, geraniol, citronellyl acetate, limonene, α-terpinene, α-terpinolen, *b*-phellandrene, *p*-cymene, carvacrol, thymol, trans-pinocarveol, α-terpineol, carvone, pinocarvone, piperitone, trans-pinocarveylhydroperoxide (TPCHP), ascaridole, isoascaridole, dihydroascaridole, caryophyllene oxide,δ3-carene,δ4-carene, camphor, apiole, and chenopanone), sesquiterpenoids (β-caryophyllene and γ-curcumene), and carotenoid terpenoids (α-carotene and *b*-carotene) [6]. The principal components in the essential oil from *C. ambrosioides* are products of monoterpenoids (C10) and sesquiterpenoids (C15), mainly ascaridole, in concentrations up to 70%, as well as limonene, trans-pinocarveyl, aritasone, β-pinene, myrcene, phellandrene, camphor, and α-terpineol. Some peroxide oxygenated alcohols were isolated from *C. ambrosioides* by extraction with n-hexane-EtOH-MeOH (1 : 1 : 1), and its structures were elucidated by NMR [7–9].

A study of phenolic compounds in *C. ambrosioides* found thirty-five compounds [10], eight of which were phenolic acids (derived from hydroxycinnamic acid). Among these, five compounds were derivates of p-coumaric acid. The other three were identified as derivates of ferulic acid. The rest of the phenolic compounds are flavones and flavonols, most of them being derivates of quercetin and kaempferol. The flavonoids were the most abundant phenolic compounds (quercetin 46.98% and kaempferol 45.91%), followed by phenolic acids (6.58%). The phenolic compounds are known by their high antioxidant activity [11, 12]. Their role as antioxidants could follow several mechanisms, including hydrogen donation reactions, metal chelation and overregulation, or protection of antioxidant defense (levels of intracellular glutathione). The aqueous extracts of *C. ambrosioides* are rich in polyphenols. The chemical composition in lipophilic compounds (fatty acids and tocopherols) was also analyzed by Barros et al. [10]. More than 26 fatty acids were identified and quantified. Polyunsaturated fatty acids predominated over saturated and monounsaturated ones. The α-linolenic and linoleic acids contributed to the high levels of polyunsaturated fatty acids (68.44%) [13].

Biosynthesis of nanoparticles from plants seems to be a very effective method of developing a rapid, clean, nontoxic, and ecofriendly technology. Furthermore, phytosynthesis

is truly a "green" synthesis route in comparison to other known methods of nanoparticle synthesis. It is evident from many reports that plants have been exploited successfully for rapid extracellular biosynthesis of metal nanoparticles [14, 15]. The potential of plants is yet to be utilized in full throttle for synthesizing metallic nanoparticles. Plants are known to harbor a broad range of metabolites. However, more profound studies are required to understand the role of these metabolites during the nanoparticle formation and stabilization. Few scientific reports on biogenic synthesis are focused on this topic [16–18], knowledge of which is required to obtain nanoparticles within a narrow size range and to have accurate morphology control. For this reason, this study used organic extracts of *C. ambrosioides* of different polarities, which were characterized phytochemically to determine the compounds responsible for Ag nanoparticle synthesis. Moreover, quantity, size, and morphology of the particles formed were studied.

2. Materials and Methods

2.1. Procedure for Obtaining Organic Extracts. *Chenopodium ambrosioides* grows spontaneously in greenhouse chrysanthemum beds in Texcoco, Mexico. One hundred grams of mature leaves was harvested, washed three times with deionized water, and sonicated for 15 min to eliminate dust and soil. Fifty grams was cut into 0.5×0.5 cm squares with stainless steel scissors previously disinfected with 95% ethanol and placed in a hermetically sealed container to perform the extractions with organic solvents. The rest of the material was dried in an oven at 62°C for 48 h, ground in an agate mortar, and sifted through a stainless steel 20-mesh screen (20 threads per inch) to homogenize particle size. This constituted the dry plant material (DPM). Five grams of DPM and 50 g of fresh plant material (FPM) were weighed and placed separately in hermetically sealed containers containing 40 mL and 250 mL hexane, respectively. Three extractions were performed during 48 h for each organic solvent used: hexane, dichloromethane, and methanol. Each extract was evaporated in a Buchi Rotavapor R-114® until the crude extract yields of each plant material were obtained.

2.2. Preliminary Analysis of Secondary Metabolites in Crude Extracts. A preliminary analysis was done to detect the presence of secondary metabolites in the crude extracts. For the test, 1 g of DPM was placed in 10 mL solvent and 10 g FPM in 100 mL solvent (hexane, dichloromethane, or methanol). A total of six extracts were counted. These were sonicated in triplicate for 15 min and filtered through Whatman number 40 filter paper. They were later placed in test tubes for the preliminary tests, which were conducted following the methodology reported by Harborne [19], adding Dragendorff reagents (alkaloids), Liebermann-Burchard (triterpenes), 3% $FeCl_3$ (phenolic compounds), Folin and NaOH (tannins), and magnesium tape and HCl (flavonoids) to 1 mL extract.

2.3. Thin-Layer Chromatography of Crude Extracts. Positive tests in the preliminary results of secondary metabolites

were subjected to chromatographic analysis. The extracts (methanol, dichloromethane, and hexane) were concentrated in a 5 mL beaker. Four chromatographic chambers were soaked with the following elution media: three chambers with ethyl acetate : methanol (7 : 3) for flavonoids, phenol compounds, and tannins and one chamber with hexane : ethyl acetate (8 : 2) for terpenoids. The extracts were applied to the chromatograph plate with silica gel, and the chromatograph developed. The plates were left to dry and observed with UV light; finally, it was sprayed with the chromogen agent.

2.4. Resuspension of Organic Extracts.
The crude extracts obtained from DPM and FPM were resuspended in 250 mL deionized water. For the crude extracts of dichloromethane and hexane, 0.1% dimethyl sulfoxide was used to enhance plant material dissolution. Resuspension consisted of dissolving each crude extract using a system of continuous shaking with a magnet and a conventional hot plate at 45°C. The crude extracts in dichloromethane were centrifuged for 5 min at 3500 rpm to eliminate undissolved plant matter.

2.5. Preparation of Silver Nanoparticles.
The reagent $AgNO_3$ was acquired from Sigma-Aldrich® of Mexico. The aqueous solution of 10 mM $AgNO_3$ was prepared following Carrillo-López et al. [20]. The colloidal solutions of nanoparticles consisted of 15 mL vials containing 1 mL resuspended crude extract, 5 mL 10 mM $AgNO_3$, and 9 mL deionized water. Bioreduction was carried out at 95°C until a change in color was observed.

2.6. UV-Vis Spectrophotometry.
Bioreduction of Ag^+ ions into nanoparticles in solution was monitored through a Perkin-Elmer Lambda 40 UV-Vis spectrophotometer. Color change indicated nanoparticle formation; colloidal silver nanoparticle solutions have a yellowish color associated with the plasmon resonance phenomena. Bioreduction finalized when absorbance of the plasmon remained constant.

2.7. Infrared Spectroscopy (FTIR).
To remove all residual biomass that did not form part of the nanoparticle coating, the samples were centrifuged at 10000 rpm for 5 min. The precipitate was discarded and the supernatant was redispersed in 10 mL deionized water. The samples were lyophilized for analysis by FTIR spectroscopy with a FTIR Bruker Tensor 27 spectrometer. Scanning was done in the range of 500 to 4000 cm^{-1} at a resolution of 1 cm^{-1}.

2.8. Transmission Electron Microscopy (TEM).
Samples for TEM characterization were obtained from AgNP solutions, when absorbance stabilized. Copper grids (mesh 200) were coated with collodion (2% in amyl acetate) and carbon; then 4 μL of the sample was placed on the grid and allowed to dry in a Petri dish. Particles were observed with a transmission electron microscope (JEM-2010 JEOL) operated at 120 kV. Images were analyzed using ImageJ (Scion Corporation, version 1.45) software to estimate size distribution of synthesized particles.

TABLE 1: Yields of *C. ambrosioides* organic extracts.

Extract	Yield (%)
Methanol/dry plant material	9.966
Methanol/fresh plant material	1.519
Dichloromethane/dry plant material	1.211
Dichloromethane/fresh plant material	0.237
Hexane/dry plant material	2.690
Hexane/fresh plant material	0.524

3. Results and Discussion

3.1. Organic Extract Yield.
Sousa et al. [21] reported extract yields obtained from dry *C. ambrosioides* shoots with 2.4% hexane, 2.94% dichloromethane, 5.4% ethyl acetate, and 5.53% ethanol. Taking the dry plant material as the reference, the highest extract yield was obtained in methanol (Table 1), similar to that obtained by Sousa et al. [21] in ethanol. Yield obtained with hexane was also similar to that reported by Sousa et al. [21]. The lowest yield was obtained with dichloromethane, contrasting with Sousa et al. [21], who found a higher extract yield with dichloromethane than with hexane. Yield is higher in dry extracts because contact area with the solvent is larger when plant material is ground to a smaller particle size.

3.2. Preliminary Test of Secondary Metabolites.
Figure 1 presents the results of the analysis of the extracts with chromogen agents, which are substances that form precipitates or foam or change in color. The hexane extracts have a straw-yellow coloring, while the dichloromethane extracts have varying colors depending on the dry (lime green) or fresh (yellowish green) plant material, and methanol extracts have an intense green tone.

Hegazy and Farrag [22] report phytochemical test on *C. ambrosioides*, in which the presence of the following chemical constituents was evidenced: volatile matter (medium presence), carbohydrates and/or glucosides (medium presence), alkaloids and/or nitrogen bases (medium presence), free and combined flavonoids (high presence), sterols and/or triterpenes (high presence), free and combined anthraquinones (high presence), saponins (absent), and tannins (absent). These results are similar to presence of these metabolites in *C. ambrosioides* organic extracts reported in Table 2. However, results of the alkaloid and tannin tests are contradictory because of the sensitivity of the methodologies and/or the different species used in the studies. Other authors have reported the presence of tannins in *C. ambrosioides* ethanol extracts [21] and isolation of saponins [23] and alkaloids [24]. Tests for esters and terpenes in *C. ambrosioides* essential oil revealed a chemical constitution of 14.6% α-terpinene, 3.6% limonene, and 18.6% ascaridole, respectively [22].

From a phytochemical viewpoint, plants pertaining to the genus *Chenopodium* have been reported to contain primary metabolites (carbohydrates, amino acids, nonpolar constituents, proteins, cytokinins, and hormones) and secondary

TABLE 2: Preliminary analysis of secondary metabolites in *C. ambrosioides* organic extracts.

Extracts	Alkaloids	Terpenoids	PC[7]	Tannins	Flavonoids	Saponins
HS[1]	−	+	−	−	−	
HF[2]	−	+	−	−	−	
DS[3]	−	++	−	+	−	
DF[4]	−	++	−	+	−	
MS[5]	−	+++	+++	++	++	−
MF[6]	−	+++	++	+++	++	−

[1]Hexane-dry plant material. [2]Hexane-fresh plant material. [3]Dichloromethane-dry plant material. [4]Dichloromethane-fresh material. [5]Methanol-dry plant material. [6]Methanol-fresh plant material. [7]Phenolic compounds.
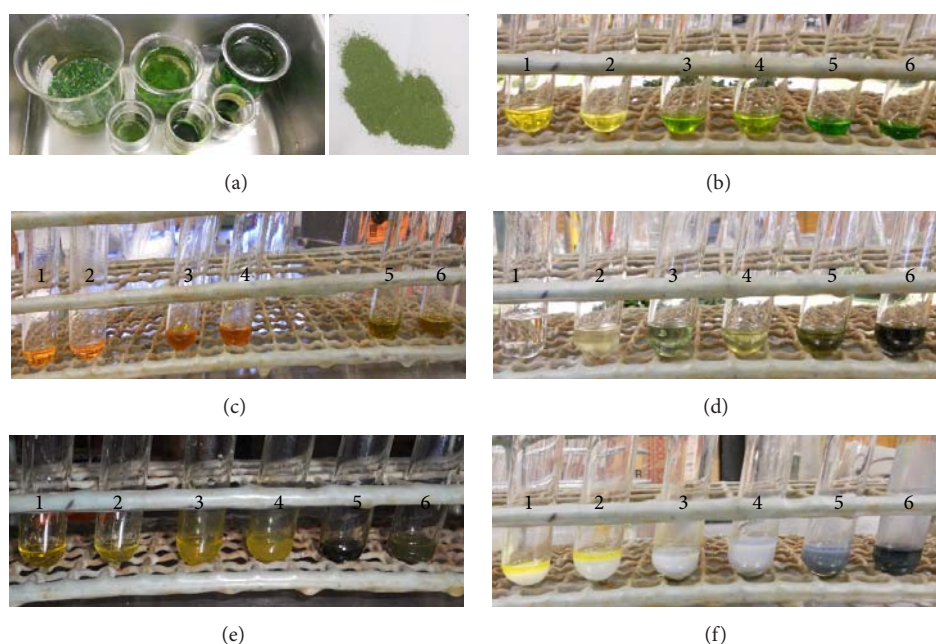

FIGURE 1: Qualitative analysis of secondary metabolites in *C. ambrosioides*. ((a) and (b)) Organic extracts obtained, (c) alkaloids, (d) triterpenes, (e) phenolic compounds, and (f) tannins; 1: hexane-dry plant material, 2: hexane-fresh plant material, 3: dichloromethane-dry plant material, 4: dichloromethane-fresh plant material, 5: methanol-dry plant material, and 6: methanol-fresh plant material.

metabolites (flavonoids, saponins, terpenes, sterols, and alkaloids). Figure 1(c) illustrates the color changes that occurred in the evaluated extracts. There was no brown precipitate, an indicator of the presence of alkaloids, confirming the negative results of the test for alkaloids in Table 2. Figure 1(d) shows a pink-purple coloring, which reveals the presence of triterpenes in the extracts. The intense coloring in the materials in methanol indicates an abundance of this type of metabolites (+++ in Table 2). Kokanova-Nedialkova et al. [6] report a vast wealth of monoterpenoids and sesquiterpenoids in *C. ambrosioides*, including β-caryophyllene, γ-curcumene, *b*-myrcene, *cis-b*-ocimene and trans-isomer, nerol, geraniol, citronellyl acetate, limonene, α-terpinene, α-terpinolen, and *b*-phellandrene. Figure 1(e) shows the color change to violet, indicating the presence of phenolic compounds, testing positive for extracts in methanol and negative for the extracts in hexane and dichloromethane. Figure 1(f) presents the typical blue coloring of extracts rich in tannins, which is

evident in the materials in methanol (particularly methanol-fresh material). The presence of flavonoids is evident in the extracts in methanol (Table 2). The presence of numerous flavonoids, such as flavone glycoside, kaempferol, kaempferol diglycoside, and kaempferol triglycoside, has been reported in *C. ambrosioides*[6]. A preliminary qualitative analysis of *C. ambrosioides* extracts obtained by Sousa et al. [21] revealed the presence of phenolic compounds, tannins, flavonoids and steroids for the ethanol extract, and flavonoids and steroids for the extract in dichloromethane.

3.3. Thin-Layer Chromatography. The chromatographic plates confirmed the presence of the compounds obtained by preliminary analysis of secondary metabolites (Figure 2). In general, an abundance of terpenoids was observed in the hexane and dichloromethane extracts, especially in dry plant material. The presence of terpenoids in the methanol extracts was minimal. However, an abundance of phenolic
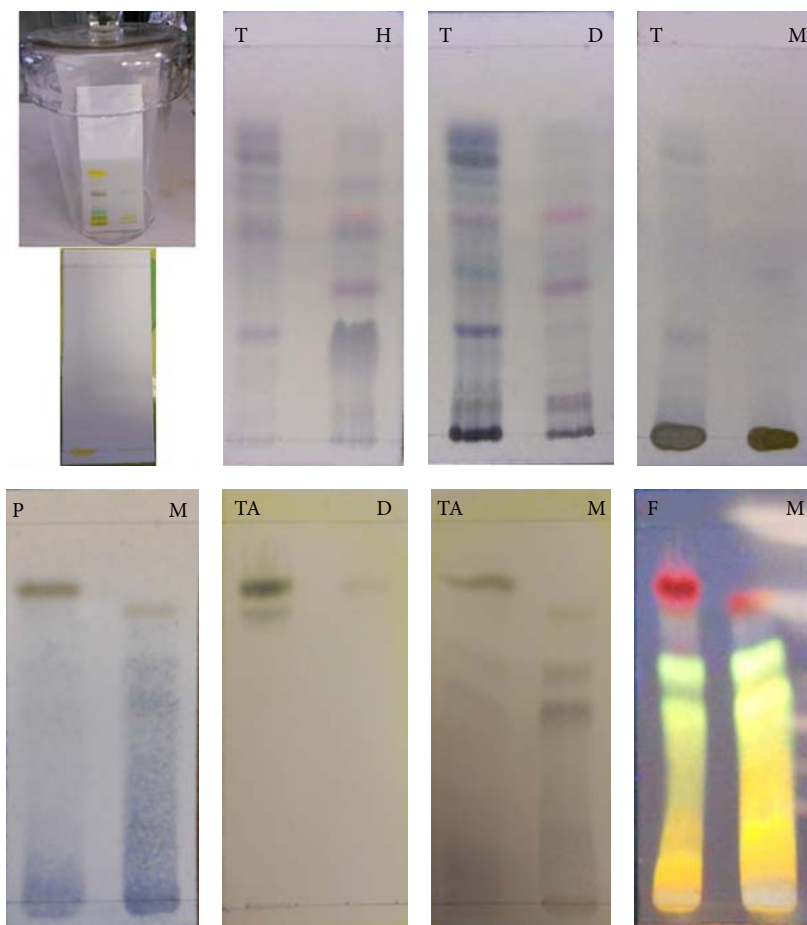
FIGURE 2: Thin-fine layer chromatography of organic *C. ambrosioides* extracts. T: terpenoids, P: phenolic compounds, TA: tannins, F: flavonoids, H: hexane, D: dichloromethane, and M: methanol. On each chromatography plate, left: dry plant material and right: fresh plant material.

compounds was observed in the methanol extracts, particularly flavonoids and tannins.

Nine classes of secondary metabolites were detected in *C. ambrosioides* chloroform extracts (sterols and terpenes, anthraquinones), ethanol (saponins), water (tannins), methanol (alkaloids), and acetone (flavonoids). The tests were positive for terpenoids, sterols, saponins, tannins, alkaloids, flavonoids, phenols, and volatile oils [25].

3.4. Color Change Associated with Particle Formation.
Particle formation was evidenced by color change of the colloidal solutions. The Ag nanoparticles exhibit colors from straw-yellow to dark brown in aqueous solutions because of the excitation caused by plasmonic surface vibrations. Figure 3 shows the color changes characteristic of the evaluated treatments. A diversity of tones was observed associated with morphological characteristics and size of the particles formed. Among the fascinating properties of metal nanoparticles (NPs) is the appearance of characteristic localized surface plasmons, whose quantum nature is a direct consequence of the small NP size, of the development of well-defined crystalline nanofacets, and of the fact that most of their atoms

are on the surface. Surface plasmons are collective excitations of the electrons at the interface between a conductor and an insulator and are described by evanescent electromagnetic waves that are not necessarily located at the interface [26]. The electrons on the surface are thus capable of interacting with electromagnetic radiation in a very complex way that is highly dependent on the shape, size, crystallinity, and chemical nature of the NPs as well as on the physical and chemical conditions of the surrounding environment [27]. During reduction of Ag+ ions to Ag nanoparticles with extracts of *Solanum trilobatum*, *Syzygium cumini*, *Centella asiatica,* and *Citrus sinensis* a color change of the solution from yellow to dark brown was observed, indicating the formation of particles [28].

3.5. Spectrophotometry UV-Vis.
Figure 4 shows the UV-Vis spectra of Ag nanoparticles synthesized with organic extracts of *C. ambrosioides*. The samples had an absorption peak between 411 and 432 nm, reported in diverse studies for Ag metal nanoparticles due to Surface Plasmon Resonance. Weak absorption peaks were observed around 219 nm, indicating the presence of organic compounds that interact in
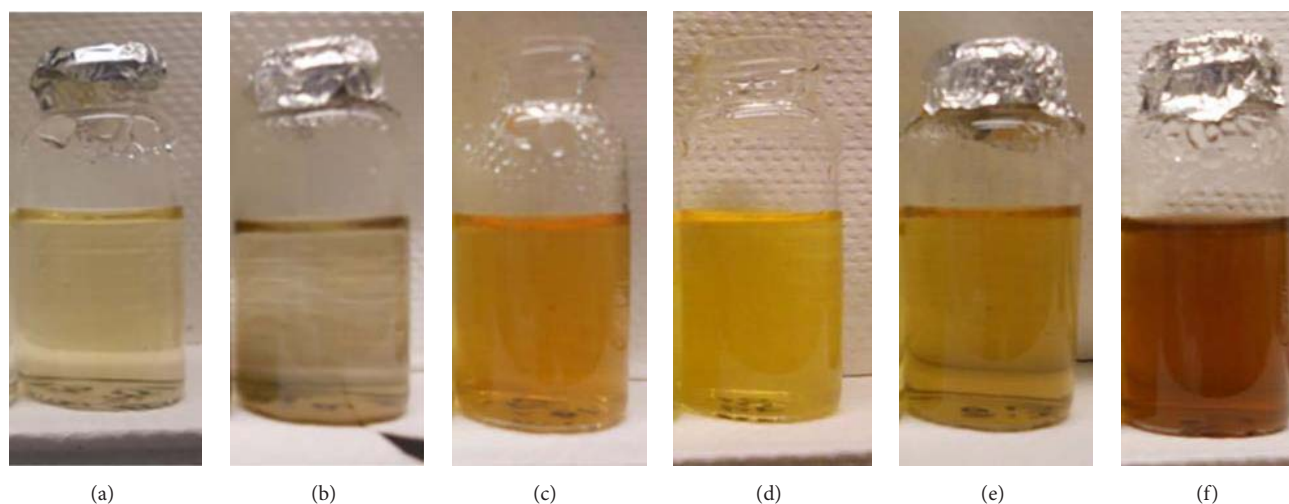
(a)   (b)   (c)   (d)   (e)   (f)

FIGURE 3: Color change of colloidal solutions of Ag nanoparticles synthesized from organic extracts of *C. ambrosioides* and 10 mM AgNO$_3$. (a) Hexane-dry plant material (DPM), (b) hexane-fresh plant material (FPM), (c) dichloromethane-DPM, (d) dichloromethane-FPM, (e) methanol-DPM, and (f) methanol-FPM.
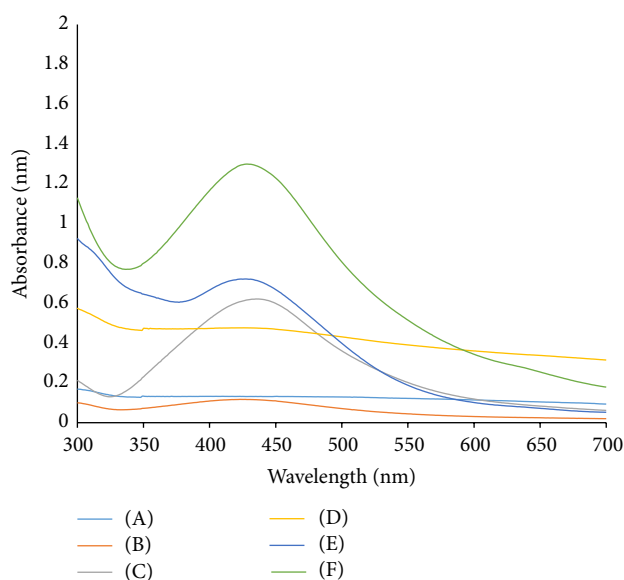

FIGURE 4: UV-Vis spectra of silver nanoparticles synthesized with extracts of (A) hexane-dry plant material (DPM), (B) hexane-fresh plant material (FPM), (C) dichloromethane-DPM, (D) dichloromethane-FPM, (E) methanol-DPM, and (F) methanol-FPM of *C. ambrosioides*, at 95°C.

solution with Ag ions in the reduction mechanism. Similar results have been reported for Ag nanoparticle synthesis with *Ananas comosus*[29].

Absorbance values are higher for the methanol extracts (Figures 4(E) and 4(F)), followed, in descending order, by the dichloromethane (Figures 4(C) and 4(D)) and hexane (Figures 4(A) and 4(B)) extracts. Therefore, there is evidence that the most powerful reducing and stabilizing molecules of the particles, of polar character, are found in the methanol

extracts. The phytochemical techniques reported previously observe that metabolites associated with methanol extracts are phenolic compounds, particularly flavonoids and tannins. That the dichloromethane extracts are also strong reducers for the formation of particles is also of immediate interest. Phytochemical studies revealed a constitution of terpenoid-type metabolites in these extracts. Although the absorbance values of hexane extracts are too low, there is also evidence of particle formation; these extracts are rich in terpenoid-type compounds in lower quantities compared to the dichloromethane extracts, as observed in the chromatographic plates in Figure 2.

The use of fresh and/or dry plant material for the extractions with solvents is also a critical point to consider for particle synthesis. Many studies do not have strict control of the origin of the plant material for biosynthesis and, in many cases, fresh plant material is used. However, this study reveals that the use of ground dry plant material has advantages. One advantage is that there is greater contact between the plant material and the solvent. In addition, the use of standard temperatures when drying the material in an oven (63–65°C) does not risk damaging the metabolites responsible for particle reduction and stabilization. Figure 4(A), showing the highest absorbances for the extractions in hexane obtained from dry plant material, can be compared with Figure 4(B), showing low absorbance values and spectra that are too wide. Absorbance values observed for dichloromethane extracts obtained with dry plant material are far from those obtained with fresh plant material. In general, extracts obtained with fresh leaves have higher absorbance values and less broad spectra. For methanol extracts, there was a similar trend.

UV-Vis spectra provide information on synthesized particles, particularly size, shape, and dispersity. Besides the influence of nanoparticle morphology such as size and shape, the physical-chemical environment also modifies Surface Plasmon Resonance (SPR) [30]. It has been shown that SPRs

shift if the dielectric properties of the surrounding media are changed. In particular, the SPRs in a medium with $n > 1$ are red-shifted with respect to those in vacuum [26]. Metal nanoparticles with a smaller number of faces and more acute vertices create resonances in a broader spectrum of wavelengths. When a nanoparticle is truncated, the principal absorption is displaced to blue, secondary resonances overlap, and, therefore, the total width increases to half of the maximum. For dodecahedral particles, truncation exhibits the same change to blue, but width decreases, possibly because the secondary resonances no longer exist when the number of faces increases [26]. Figure 4(B) shows wide spectra for the different concentrations of silver evaluated, suggesting that they are large polydisperse particles with truncated shapes. Although broad spectra are not observed in spectra (E), Figure 4 shows that the shape of the spectra is not symmetrical; the left side is cut off, and, therefore, the information of the particles they provide is that they are more polyhedral in shape and less truncated but polydisperse. Figures 4(C), 4(E), and 4(F) present spectra with symmetrical shapes and acute angles. For this reason, it would be expected that the synthesized particles possess little polydispersity and are small and polyhedral-shaped, desirable characteristics for nanoparticle synthesis.

3.6. Transmission Electron Microscopy. In the hexane extracts, diversely shaped particles are observed (Figure 5), in particular in the hexane-fresh plant material extract. This may be due to the fact that there are few molecules to coat the reduced particles (capping) causing coalescence produced by larger irregularly shaped particles [5, 20]. Figures 5(d) and 5(e) show little disparity in particle size, which coincides with the acute shape and symmetry in the spectra shown in Figures 4(C) (dichloromethane-dry plant material extract) and 4(F) (methanol-fresh plant material extract). Therefore, in dichloromethane extracts we should use dry plant material, while in methanol extracts it is recommendable to use fresh plant material. The compounds of polar character (extracted with methanol) lose reducing activity during the process of drying the plant material; among these are phenolic compounds (flavonoids and tannins). In contrast, the terpenoids (extracted with dichloromethane and hexane) are less affected during plant material processing. The distribution of particle size (Figure 6) shows small nanoparticles obtained with low polydispersity (Figures 6(c) and 6(f)) in dichloromethane and methanol extracts. However, in the hexane extracts, particle sizes are large (Figures 6(a) and 6(b)). With the results shown in Figures 4 and 5, we conclude that the smallest particles are obtained with extracts in dichloromethane-dry plant material and methanol-fresh plant material.

3.7. Infrared Spectroscopy. Figures 7, 8, and 9 show the infrared spectra for the organic extracts in hexane, dichloromethane, and methanol, before and after bioreduction. The information obtained from the bands or "peaks" helps to elucidate the compounds responsible for particle reduction and stabilization by means of the functional groups found. Differences in the extract before and after synthesis can

be observed. Figure 7(a) corresponds to extracts in hexane with dry plant material before bioreduction (Figure 7(a)(A)). Absorption bands are produced at $2852\,cm^{-1}$ and $1741\,cm^{-1}$, which are associated with the CH group and the carbonyl group in aldehydes; after reduction of the Ag ions, aldehydes are oxidized to carboxylic acids, increasing bands $3389\,cm^{-1}$ and $1272\,cm^{-1}$, which correspond to the –OH group and the carbonyl group of carboxylic acids, respectively.

Figure 7(b) shows the spectra before and after reduction with fresh plant extract. In this case, we observe a similarity in the bands that appear in Figure 7(a), resulting in aldehyde oxidation to carboxylic acids for reducing Ag ions. It is likely that the aldehydes come from oxidation of the hydroxyl groups contained in the hexane extract metabolites. The metabolites extracted in hexane are predominantly terpenoids (Figure 2). Some that are reported for *C. ambrosioides* have hydroxyl groups in their structure and, therefore, reducing power; these include nerol, geraniol, carvacrol, thymol, trans-pinocarveol, trans-diol, monoterpene hydroperoxides, and tocopherols. According to Kagan et al. [31], α-tocopherol was more abundant in *C. ambrosioides* (199.37 mg/100 g dry weight). The tocopherols are natural antioxidants, especially those rich in polyunsaturated fatty acids. Their effectiveness as antioxidants depends not only on their reactivity against radicals but also on the stable nature of their radicals due to the relocation of the unpaired electron on the chromane ring [31].

Figures 8(a) and 8(b) show the infrared spectra for dichloromethane extracts before (A) and after bioreduction (B). In this case, a trend is observed in the appearance of the peaks similar to those appearing in hexane extracts. Figure 2 shows a wealth of terpenoid-type metabolites, even more abundant than in the hexane extracts. Absorption bands are observed at $2852\,cm^{-1}$ and $1741\,cm^{-1}$, associated with the CH group and the carbonyl group in aldehydes, respectively. After reduction of the Ag ions, aldehydes oxidize into carboxylic acids, observing an increase of the band of $1298\,cm^{-1}$, corresponding to the carbonyl group of carboxylic acids. Again, the aldehyde groups should originate from oxidation of the hydroxyl groups contained in the structure of the terpenoids. *Chenopodium ambrosioides* oil has been shown to have antioxidant, antifungal, and antiaflatoxigenic activity [32]. *Chenopodium* oil is a mixture of ascaridole (55.3%), *p*-cymene (16.2%), α-terpinene (9.7%), isoascaridole (4.3%), and limonene (3.8%). Strong antioxidant activity of a concentration of $3000\,\mu g/mL$ was found, comparable to ascorbic acid (used as reference). Other authors have reported that *C. ambrosioides* oil contains α-terpinene, *p*-cymene, carene, and ascaridole, while others have reported α-pinene, *b*-phellandrene, and limonene as majority compounds. The antioxidant activity of *C. ambrosioides* essential oils could be attributed to the presence of compounds such as estragole, thymol, and carvacrol, which, although their amounts are small, exert antioxidant activity as radical capturers. Moreover, hydrocarbons of monoterpene and sesquiterpene nature act in a way similar to α-terpinene. For this reason, the essential oils that do not contain phenolic compounds in their composition can act as antioxidants [33].
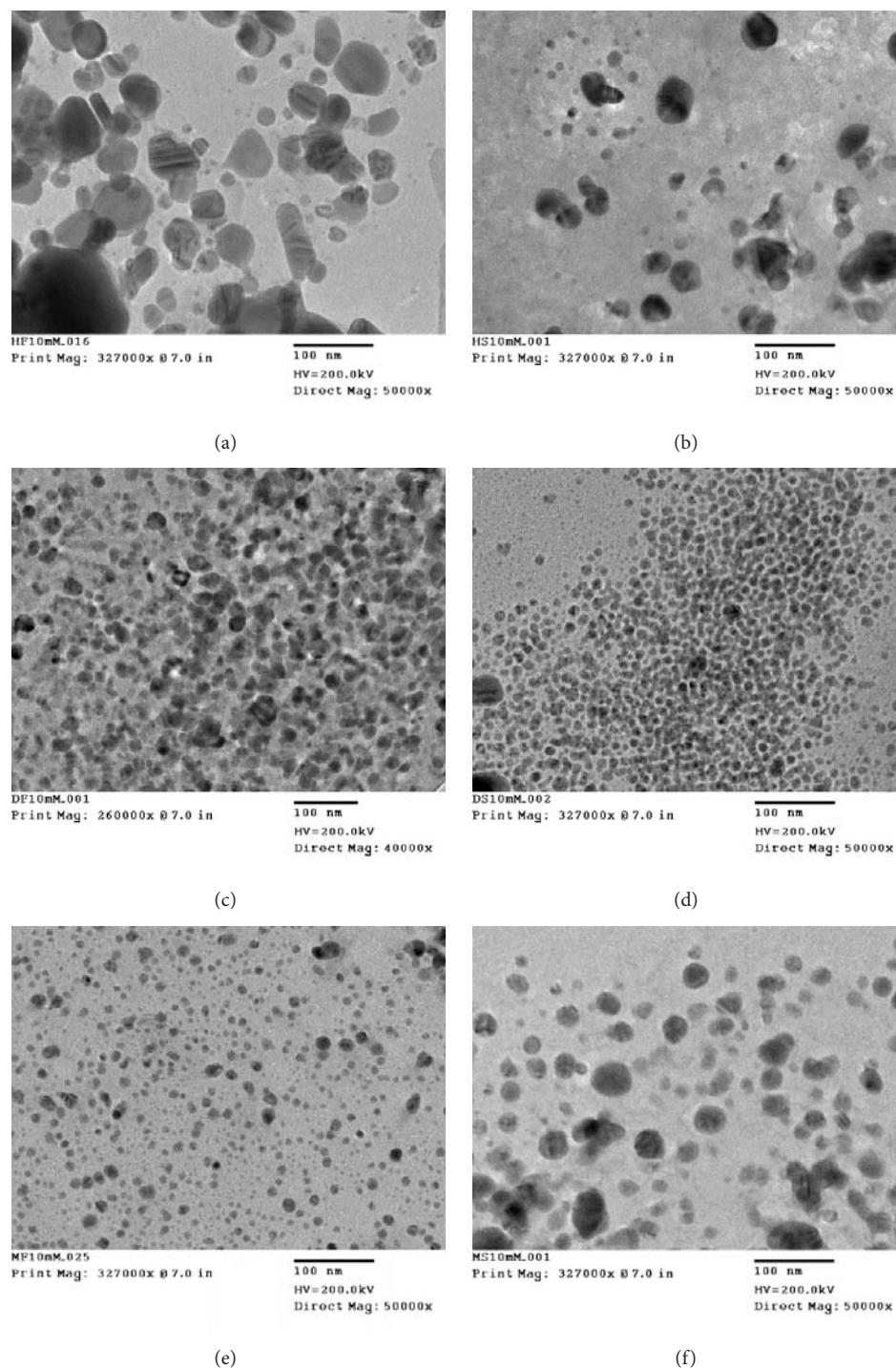
(a)

(b)

(c)

(d)

(e)

(f)

FIGURE 5: Transmission electron micrographs of AgNPs synthesized from organic extracts of *Chenopodium ambrosioides* and 10 mM AgNO$_3$. (a) Hexane-fresh plant material (FPM), (b) hexane-dry plant material (DPM), (c) dichloromethane-FPM, (d) dichloromethane-DPM, (e) methanol-FPM, and (f) methanol-DPM.

Figures 9(a) and 9(b) show the infrared spectra before (A) and after bioreduction (B) with extracts in methanol. Before bioreduction (Figure 9(a)), the spectrum marked with the letter "A" has an absorbance band at 3359 cm^{-1}, associated with stretching vibration and deformation of C–O–H in phenols. The "B" line represents the infrared absorption spectrum after bioreduction. Here, the 3359 signal disappears because of Ag$^+$ ion reduction. The increase in the absorption band at 1391 cm^{-1} is associated with the –COO group, which participates in nanoparticle stabilization. The band that appears after bioreduction at 800 cm^{-1} is associated with –CH in substituted benzenes bound to carboxylate
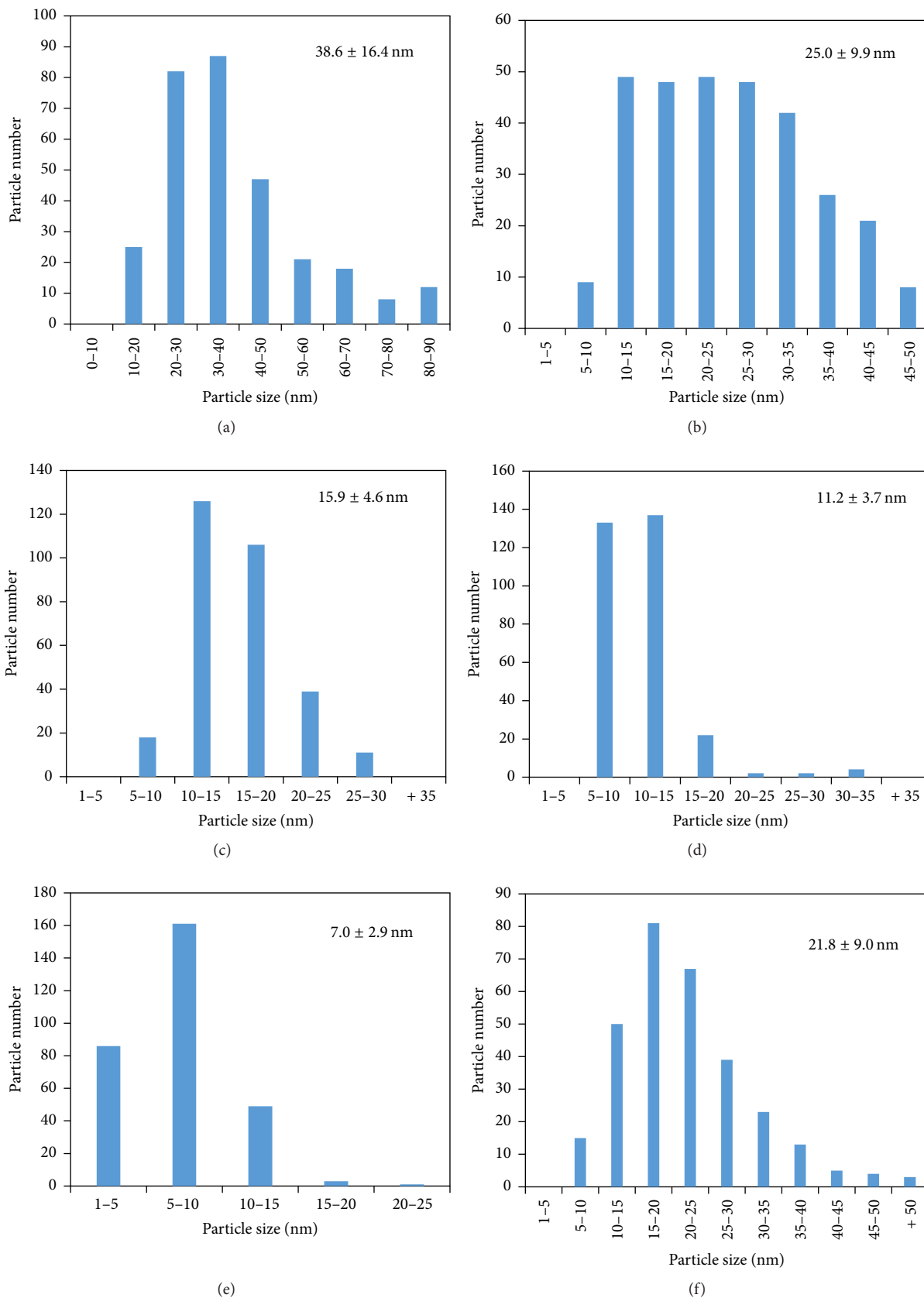
Figure 6: Histograms of size distribution of AgNPs synthesized from organic extracts of *Chenopodium ambrosioides* and 10 mM AgNO$_3$. (a) Hexane-fresh plant material (FPM), (b) hexane-dry plant material (DPM), (c) dichloromethane-FPM, (d) dichloromethane-DPM, (e) methanol-FPM, and (f) methanol-DPM. The insert corresponds to mean ± SD of size particle.
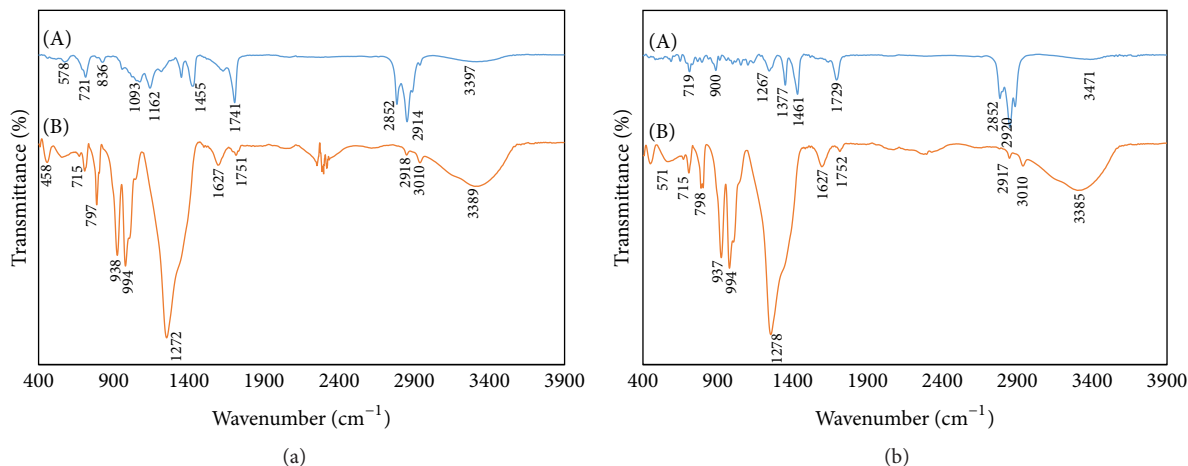
Figure 7: FTIR absorbance spectra of extracts in hexane before (A) and after (B) bioreduction of silver ions. (a) Dry and (b) fresh *C. ambrosioides* plant material.
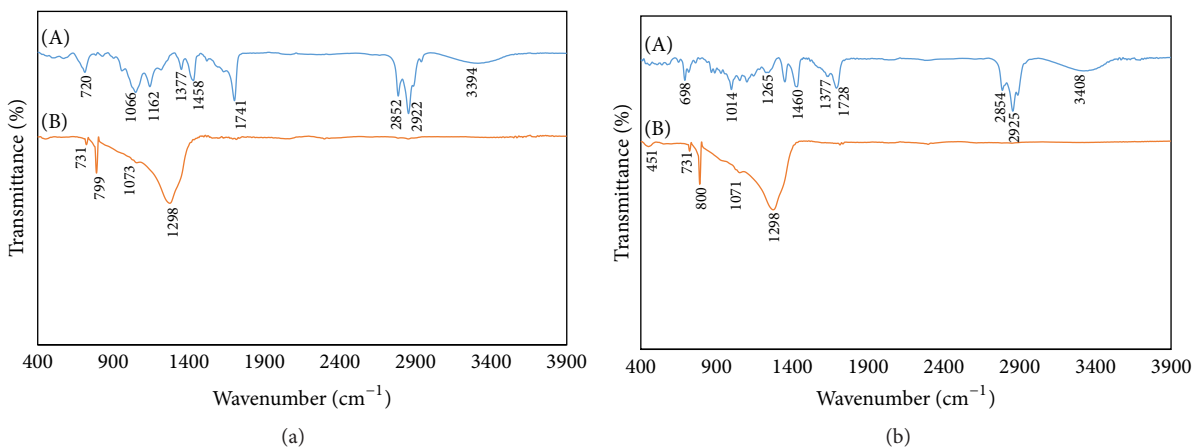

Figure 8: FTIR absorbance spectra of extracts in dichloromethane before (A) and after (B) bioreduction of silver ions. (a) Dry and (b) fresh *C. ambrosioides* plant material.
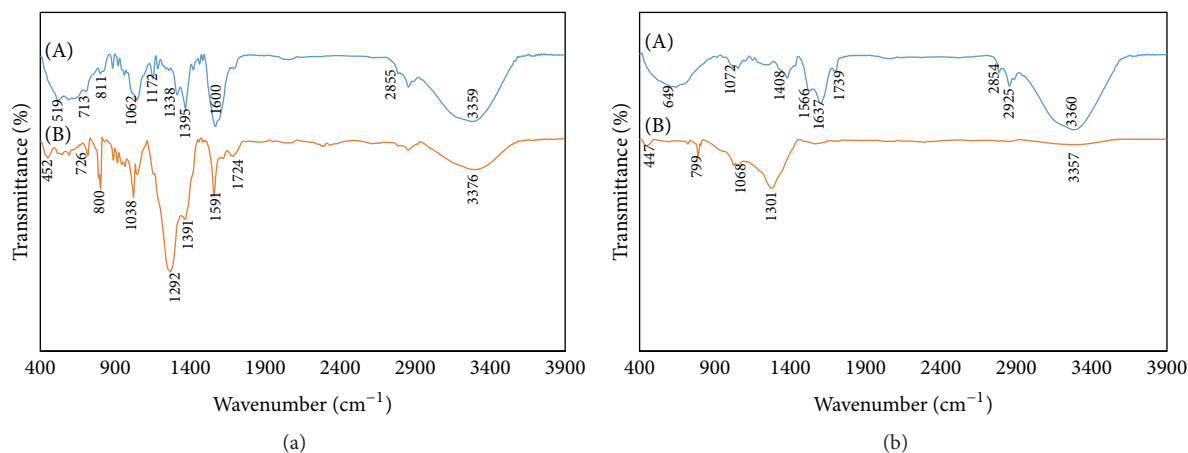

Figure 9: FTIR absorbance spectra of extracts in methanol before (A) and after (B) bioreduction of silver ions. (a) Dry and (b) fresh *C. ambrosioides* plant material.

groups. Bioreduction studies with *Chenopodium album* have reported participation of carbonyl groups in the Ag$^+$ ion reduction process and carboxylate ions as stabilization agents in nanoparticles synthesized over time [34]. In contrast, some authors report that –OH groups participate in the reduction process, oxidizing the –OH groups to carbonyl groups, and carbonyl and carboxylate groups are involved in particle stabilization [34, 35].

Many authors name flavones, terpenoids, and polysaccharides as responsible for bioreduction. In our study with *C. ambrosioides*, the disappearance of the –OH group after bioreduction makes it evident that this functional group is responsible for reduction of silver ions [35]. Phytochemical characterization of *C. ambrosioides* methanol found that the principal metabolites were phenolic compounds (flavonoids and tannins) and a smaller proportion of terpenoids.

Barros et al. [10] evaluated bioactivity and characterized hydrophilic and lipophilic compounds of *C. ambrosioides*. The bioactive properties include antioxidant and antitumor activity and hepatotoxicity. The aqueous extracts are more active against free radicals, bleaching β-carotene, and inhibiting TBARS (inhibition of lipid peroxidation by decreasing thiobarbituric acid reactive substances) than extracts in methanol. They also have higher reducing activity. *C. ambrosioides* essential oils from leaves also show antioxidant activity. Aqueous extracts of *C. ambrosioides* did not exhibit antitumor potential, but the extracts in methanol did. Organic acids, such as citric acid, have been reported to possess antioxidant activity [36].

Yoosaf et al. [37] found that a molecule should have at least two hydroxyl groups in *ortho-* or *para*-position to produce ion reduction. The dihydroxyl compounds of gallic acid oxidize to a quinone, and the nanoparticles formed stabilize with interaction of the carboxylic acid group.

Rodríguez-León et al. [38] found that the Ag$^+$ ion reducing agents were the organic molecules of epicatechin and epicatechin gallate, found by nuclear magnetic resonance in extracts of *R. hymenosepalus*. The reducing mechanism involves abstraction of hydrogen because of the OH groups in polyphenol molecules.

In the methanol extracts, the phenolic compounds with hydroxyl groups include flavone glycosides, quercetin, kaempferol, and their glycosides and isorhamnetin, in particular, flavone glycoside, which has two hydroxyl groups in its structure. The terpenoids found in the extracts in hexane and dichloromethane that have two hydroxyl groups include monoterpene hydroperoxides, apiole, α-terpineol, and related derivates, trans-diol, (−)-(1R, 2S, 3S, 4S)-1,2,3,4,-tetrahydroxy-p-menthane, avenasterol, and α-spinasterol.

Conventional phytochemical tests conducted on dry *Citrus sinensis* plant material produced positive results for alkaloids, tannins, flavonoids, and steroids. *C. sinensis* and *Syzygium cumini* (positive for flavonoids) produce higher absorbance values in UV-Vis spectrophotometry than *Solanum trilobatum* (positive for alkaloids, tannins, and steroids) and *Centella asiatica* (positive for tannins and steroids). This indicates that flavonoids are the metabolites with greater Ag$^+$ ion reducing power and particle stabilization for these cases [28, 37].

4. Conclusions

This is the first study to elucidate the organic compounds of *Chenopodium ambrosioides* that participate in bioreduction of Ag nanoparticles. The strategy was based on the study of biosynthesis in extracts of different polarities (high with methanol, medium with dichloromethane, and low with hexane). The extracted metabolites were assessed and the organic compounds were analyzed before and after bioreduction (FTIR technique). The extracts in methanol, rich in phenolic compounds (flavonoids and tannins), have greater reducing and stabilizing activity for Ag nanoparticle synthesis. Nevertheless, the terpenoids present in the dichloromethane and hexane extracts also have reducing activity, though in lower proportion. Large part of the reducing activity of the secondary metabolites in *C. ambrosioides* is favored by the compounds that have antioxidant capacity, including the phenolic compounds (flavone glycoside and isorhamnetin) and terpenoids (trans-diol, α-terpineol, and derivatives, monoterpene hydroperoxides and apiole). Dry plant material is more efficient in the production of Ag nanoparticles when working with hexane and dichloromethane extracts. However, when working with methanol, fresh plant material should be used.
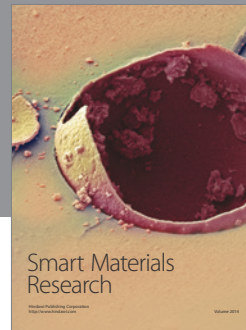
Competing Interests

The authors declare that there is no conflict of interests regarding the publication of this manuscript.

References

[1] S. S. Shankar, A. Rai, A. Ahmad, and M. Sastry, "Rapid synthesis of Au, Ag, and bimetallic Au core-Ag shell nanoparticles using Neem (*Azadirachta indica*) leaf broth," *Journal of Colloid and Interface Science*, vol. 275, no. 2, pp. 496–502, 2004.

[2] N. Yadav, N. Vasudeva, S. Singh, and S. K. Sharma, "Medicinal properties of genus *Chenopodium* Linn.," *Indian Journal of Natural Products and Resources*, vol. 6, no. 2, pp. 131–134, 2007.

[3] R. Villase and G. Espinosa, *Catálogo de malezas de México*, Consejo Nacional Consultivo Fitosanitario, Fondo de Cultura Económica, Mexico City, Mexico, 1998.

[4] N. Ramezani, Z. Ehsanfar, F. Shamsa et al., "Screening of medicinal plant methanol extracts for the synthesis of gold nanoparticles by their reducing potential," *Zeitschrift für Naturforschung B*, vol. 63, no. 7, pp. 903–908, 2008.

[5] J. Y. Song and B. S. Kim, "Biological synthesis of bimetallic Au/Ag nanoparticles using Persimmon (*Diopyros kaki*) leaf extract," *Korean Journal of Chemical Engineering*, vol. 25, no. 4, pp. 808–811, 2008.

[6] Z. Kokanova-Nedialkova, P. T. Nedialkov, and S. D. Nikolov, "The genus *Chenopodium*: phytochemistry, ethnopharmacology and pharmacology," *Pharmacognosy Reviews*, vol. 3, no. 6, pp. 280–306, 2009.

[7] M. A. Johnson and R. Croteau, "Biosynthesis of ascaridole: iodide peroxidase-catalyzed synthesis of a monoterpene endoperoxide in soluble extracts of *Chenopodium ambrosioides* fruit," *Archives of Biochemistry and Biophysics*, vol. 235, no. 1, pp. 254–266, 1984.

[8] A. A. Ahmed, "Highly oxygenated monoterpenes from *Chenopodium ambrosioides*," *Journal of Natural Products*, vol. 63, no. 7, pp. 989–991, 2000.

[9] F. Kiuchi, Y. Itano, N. Uchiyama et al., "Monoterpene hydroperoxides with trypanocidal activity from *Chenopodium ambrosioides*," *Journal of Natural Products*, vol. 65, no. 4, pp. 509–512, 2002.

[10] L. Barros, E. Pereira, R. C. Calhelha et al., "Bioactivity and chemical characterization in hydrophilic and lipophilic compounds of *Chenopodium ambrosioides* L.," *Journal of Functional Foods*, vol. 5, no. 4, pp. 1732–1740, 2013.

[11] E. González de Mejía, Y. S. Song, C. I. Heck, and M. Ramírez-Mares, "Yerba mate tea (*Ilex paraguariensis*): phenolics, antioxidant capacity and *in vitro* inhibition of colon cancer cell proliferation," *Journal of Functional Foods*, vol. 2, no. 1, pp. 23–34, 2010.

[12] O. R. Pereira, R. I. R. Macías, M. J. Pérez, J. J. G. Marín, and S. M. Cardoso, "Protective effects of phenolic constituents from *Cytisus multiflorus, Lamium album* L. and *Thymus citriodorus* on liver cells," *Journal of Functional Foods*, vol. 5, no. 3, pp. 1170–1179, 2013.

[13] J. Whelan, "The health implications of changing linoleic acid intakes," *Prostaglandins, Leukotrienes and Essential Fatty Acids*, vol. 79, no. 3–5, pp. 165–167, 2008.

[14] K. Quester, M. Avalos-Borja, and E. Castro-Longoria, "Biosynthesis and microscopic study of metallic nanoparticles," *Micron*, vol. 54-55, pp. 1–27, 2013.

[15] M. S. Akhtar, J. Panwar, and Y.-S. Yun, "Biogenic synthesis of metallic nanoparticles by plant extracts," *ACS Sustainable Chemistry & Engineering*, vol. 1, no. 6, pp. 591–602, 2013.

[16] M. S. Akhtar, M. K. Swamy, A. Umar, and A. A. Al Sahli, "Biosynthesis and characterization of silver nanoparticles from methanol leaf extract of cassia didymobotyra and assessment of their antioxidant and antibacterial activities," *Journal of Nanoscience and Nanotechnology*, vol. 15, no. 12, pp. 9818–9823, 2015.

[17] M. R. Chitsazi, H. Korbekandi, G. Asghari, R. Bahri Najafi, A. Badii, and S. Iravani, "Synthesis of silver nanoparticles using methanol and dichlorometane extracts of *Pulicaria gnaphalodes* (Vent.) Boiss," *Artificial Cells, Nanomedicine, and Biotechnology*, vol. 44, no. 1, pp. 328–333, 2014.

[18] F. Azizinezhad, Z. Z. Nasrollahi, and S. Sadrnezhaad, "Synthesis of the silver nanoparticles with the using of camomile plant," *European Journal of Experimental Biology*, vol. 4, no. 2, pp. 124–127, 2014.

[19] A. Harborne, *Phytochemical Methods: A Guide to Modern Techniques of Plant Analysis*, Springer, Amsterdam, Netherlands, 1984.

[20] L. M. Carrillo-López, H. A. Zavaleta-Mancera, A. Vilchis-Nestor et al., "Biosynthesis of silver nanoparticles using *Chenopodium ambrosioides*," *Journal of Nanomaterials*, vol. 2014, Article ID 951746, 9 pages, 2014.

[21] Z. L. Sousa, F. F. de Oliveira, A. O. da Conceição et al., "Biological activities of extracts from *Chenopodium ambrosioides* Lineu and *Kielmeyera neglecta* Saddi," *Annals of Clinical Microbiology and Antimicrobials*, vol. 11, pp. 20–27, 2012.

[22] A. Hegazy and H. Farrag, "Allelopathic potential of *Chenopodium ambrosioides* on germination and seedling growth of some cultivated and weed plants," *Global Journal of Biotechnology & Biochemistry*, vol. 2, no. 1, pp. 1–9, 2007.

[23] G. Gupta and M. Behari, "Chemical investigation of *Chenopodium ambrosioides*," *Journal of Indian Chemical Society*, vol. 49, no. 3, pp. 317–319, 1972.

[24] A. Hasseb, B. Singh, A. Khan, and S. Saxena, "Evaluation of nematicidal property in certain alkaloid bearing plants," *Geobios*, vol. 5, pp. 116–118, 1978.

[25] S. Okhale, H. Egharevba, E. Ona, and O. Kunle, "Phytochemicaland proximate analyses and thin layer chromatography fingerprinting of the aerial part of *Chenopodium ambrosioides* Linn. (Chenopodiaceae)," *Journal of Medicinal Plants Research*, vol. 6, no. 12, pp. 2289–2294, 2012.

[26] C. Noguez, "Surface plasmons on metal nanoparticles: the influence of shape and physical environment," *Journal of Physical Chemistry C*, vol. 111, no. 10, pp. 3806–3819, 2007.

[27] D. Cruz, M. Rodríguez, J. López, V. Herrera, A. Orive, and A. Creus, "Metallic nanoparticles and surface plasmons: a deep relationship," *Avances en Ciencias e Ingeniería*, vol. 3, no. 2, pp. 67–78, 2012.

[28] P. Logeswari, S. Silambarasan, and J. Abraham, "Ecofriendly synthesis of silver nanoparticles from commercially available plant powders and their antibacterial properties," *Scientia Iranica*, vol. 20, no. 3, pp. 1049–1054, 2013.

[29] N. Ahmad and S. Sharma, "Green synthesis of silver nanoparticles using extracts of *Ananas comosus*," *Green and Sustainable Chemistry*, vol. 02, no. 04, pp. 141–147, 2012.

[30] C. Novo, A. M. Funston, I. Pastoriza-Santos, L. M. Liz-Marzán, and P. Mulvaney, "Influence of the medium refractive index on the optical properties of single gold triangular prisms on a substrate," *The Journal of Physical Chemistry C*, vol. 112, no. 1, pp. 3–7, 2008.

[31] V. E. Kagan, A. I. Kuzmenko, A. A. Shvedova et al., "Direct evidence for recycling of myeloperoxidase-catalyzed phenoxyl radicals of a vitamin E homologue, 2,2,5,7,8-pentamethyl-6-hydroxy chromane, by ascorbate/dihydrolipoate in living HL-60 cells," *Biochimica et Biophysica Acta (BBA)—General Subjects*, vol. 1620, no. 1–3, pp. 72–84, 2003.

[32] R. Kumar, A. K. Mishra, N. K. Dubey, and Y. B. Tripathi, "Evaluation of *Chenopodium ambrosioides* oil as a potential source of antifungal, antiaflatoxigenic and antioxidant activity," *International Journal of Food Microbiology*, vol. 115, no. 2, pp. 159–164, 2007.

[33] B. Jaramillo, E. Duarte, and W. Delgado, "Bioactividad del aceite esencial de *Chenopodium ambrosioides* colombiano," *Revista Cubana de Plantas Medicinales*, vol. 17, no. 1, pp. 54–64, 2012.

[34] A. Dhar Dwivedi and K. Gopal, "Biosynthesis of silver and gold nanoparticles using *Chenopodium album* leaf extract," *Colloids and Surfaces A: Physicochemical and Engineering Aspects*, vol. 369, no. 1–3, pp. 27–33, 2010.

[35] J. Huang, Q. Li, D. Sun et al., "Biosynthesis of silver and gold nanoparticles by novel sundried *Cinnamomum camphora* leaf," *Nanotechnology*, vol. 18, no. 10, Article ID 105104, 2007.

[36] A. R. Hraš, M. Hadolin, Ž. Knez, and D. Bauman, "Comparison of antioxidative and synergistic effects of rosemary extract with α-tocopherol, ascorbyl palmitate and citric acid in sunflower oil," *Food Chemistry*, vol. 71, no. 2, pp. 229–233, 2000.

[37] K. Yoosaf, B. I. Ipe, C. H. Suresh, and K. G. Thomas, "In situ synthesis of metal nanoparticles and selective naked-eye detection of lead ions from aqueous media," *The Journal of Physical Chemistry C*, vol. 111, no. 34, pp. 12839–12847, 2007.

[38] E. Rodríguez-León, R. Iñiguez-Palomares, R. E. Navarro et al., "Synthesis of silver nanoparticles using reducing agents obtained from natural sources (*Rumex hymenosepalus* extracts)," *Nanoscale Research Letters*, vol. 8, no. 1, pp. 1–9, 2013.